Evol Biol
DOI 10.1007/s11692-008-9045-4

RESEARCH ARTICLE

Developmental and Genetic Constraints on Neurocranial Globularity: Insights from Analyses of Deformed Skulls and Quantitative Genetics

Neus Martínez-Abadías · Carolina Paschetta · Soledad de Azevedo · Mireia Esparza · Rolando González-José

Received: 2 July 2008 / Accepted: 31 October 2008

Abstract Neurocranial globularity is one of the few derived traits defining anatomically modern humans. Variations in this trait derive from multiple and complex interactions between portions of the brain and the size and shape of the cranial base, among other factors. Given their evolutionary and functional importance, neurocranial globularity is expected to present high genetic and developmental constraints on their phenotypic expression. Here we applied two independent approaches to investigate both types of constraints. First, we assessed if patterns of morphological integration are conserved or else disrupted on a series of artificially deformed skulls in comparison to non-deformed (ND) ones. Second, after the estimation of the genetic covariance matrix for human skull shape, we explored how neurocranial globularity would respond to putative selective events disrupting the normal morphological patterns. Simulations on these deviations were explicitly set to replicate the artificial deformation patterns in order to compare developmental and genetic constraints under the same biomechanical conditions. In general terms, our results indicate that putative developmental constraints help to preserve some aspects of normal morphological integration even in the deformed skulls. Moreover, we find that the response to selection in neurocranial globularity is pervasive. In other words, induced changes in the vault generate a global response, indicating that departures from normal patterns of neurocranial globularity are genetically constrained. In summary, our combined results suggest that neurocranial globularity behaves as a highly genetic and developmental constrained trait.

Keywords Constraints · Neurocranial globularity · Quantitative genetics · Geometric morphometrics · Morphological integration · Artificial deformation

Introduction

The debate about the shared derived traits defining modern humans is classical among human biologists (Howells 1973; Wolpoff 1980; Lahr 1996; Lieberman et al. 2002; Tattersall 2002; Ackermann and Cheverud 2004; Strait et al. 2007; Rightmire 2007). Most, if not all of the synapomorphies characterizing our species, as well as other groups of vertebrates, represent continuous changes in complex structures, such as the skull, dentition, and other parts of the skeleton, and are subjected to a variety of evolutionary constraints operating at different levels (Lieberman 1997; Strait 2001; Ackermann and Cheverud 2004; Bastir and Rosas 2004, 2005). Most scholars, however, are in agreement in considering neurocranial globularity (or roundness) as one of the few derived traits defining anatomically modern humans (e.g. Day and Stringer 1982, 1991; Lieberman 1995; Ponce de León and Zollikofer

Neus Martínez-Abadías and Rolando González-José contributed equally to this work.

Electronic supplementary material The online version of this article (doi:10.1007/s11692-008-9045-4) contains supplementary material, which is available to authorized users.

N. Martínez-Abadías · M. Esparza
Secció d'Antropologia, Departament de Biologia Animal, Universitat de Barcelona. Av. Diagonal, 645. 08028 Barcelona, Spain

C. Paschetta · S. de Azevedo · R. González-José (✉)
Centro Nacional Patagónico, Consejo Nacional de Investigaciones Científicas y Técnicas (CONICET), Bvd. Brown 2825, U9120ACF Puerto Madryn, Argentina
e-mail: rolando@cenpat.edu.ar

2001; Lieberman et al. 2002; Strait and Grine 2004; Collard and Wood 2007; González-José et al. 2008).

Previous works demonstrate that neurocranial globularity is a very complex trait affected by many factors (e.g. Enlow 1990; Lieberman et al. 2002; Bastir et al. 2007; Hallgrímsson et al. 2007a, b). Like other complex structures, variations in neurocranial globularity derive from the combination of variation introduced by developmental and environmental factors interacting at different stages of development (e.g. Enlow 1990; Bastir et al. 2007; Hallgrímsson et al. 2007a, b). Several mechanisms have been proposed to explain how these interactions operate. For instance, some authors put emphasis on the mesenchymal condensations and differentiation as an important step during embryonic development that determines the shape, size and patterns of covariance among skeletal structures (Atchley and Hall 1991; Hall 2005). According to this view, variation of the genetic-based regulation of the condensation and differentiation of mesenchymal cells drive covariation of regions at different levels. Other authors propose that function is an important factor generating covariances among structures as well (Moss and Young 1960). Thus, the logic to divide the skull into modules reflecting functional demands is based on the pioneering work by Moss (1968). In the Moss' functional matrix hypothesis, the growth of the skeletal units is determined by the function of the soft tissues and functional spaces in which they are embedded. The functional matrix includes all the elements (organs, tissues, nerves, functional spaces, etc.) necessary to perform a function. According to this hypothesis, it is expected that skeletal elements that are part of the same functional matrix will be more highly integrated than they will be with traits of a different functional matrix.

In an effort to organize the way in which these and other processes operate since the formation of the zygote to the adult specimen (Hallgrímsson et al. 2007b) and Hallgrímsson and Lieberman (2008) have synthesized the sequential effects of developmental and environmental factors into a "palimpsest" model. Under this model, the covariation patterns of an adult skull can be viewed as the final result of the summed imprint of a succession of effects, each of which leaves a distinctive covariation signal by the specific set of developmental interactions involved (Hallgrímsson et al. 2007b; Hallgrímsson and Lieberman 2008). Thus, the palimpsest model attempts to sum up all the previous research concerning developmental processes responsible of covariation (e.g. neural crest migration, patterning and proliferation, facial process fusion, cell condensation and differentiation, cartilage growth, brain growth, muscle–bone interactions, somatic growth, etc.) into a framework that helps to predict the response to variations at any level in terms of adult final morphology.

Depending on their developmental origins, three main regions are usually distinguished within the skull, namely the basicranium, the neurocranium and the face (Sperber 2001). The basicranium derives from the chondrocranium, which is a cartilaginous precursor of the cranial base; the neurocranium is formed from the desmocranium, from mesodermal and neural crest cells; and finally, the face is developed from the splanchnocranium, which ossifies intramembranously like the cranial vault but only from neural crest precursors (Sperber 2001). These skull regions grow during different ontogenic times and its development is regulated after different epigenetic and genetic factors. The base is the first region to develop, followed by the cranial vault and the face (Sperber 2001). The growth of the neurocranial structures (both the base and the cranial vault) is mainly driven by the growth of the expanding brain and occurs early during the ontogeny, during the prenatal and neonatal periods, while the face develops later, once the brain has finished its growth. The face and the mandible grow during a more extended period of time, reaching its maturity at an early age (Sperber 2001).

Given its evolutionary and functional importance, and considering the complex pattern of development and integration with other cranial traits (Enlow 1990; Ackermann and Cheverud 2004; Lieberman et al. 2002, 2004; Bastir et al. 2007) neurocranial globularity is expected to present high developmental and genetic constraints on their phenotypic expression. Constraints are factors that limit evolutionary change. Constraints can be regarded in a 'negative' way since they reduce the extent of heritable phenotypic variation; that is, if there were particular combinations of traits lacking additive genetic variation, evolution in certain directions in phenotype space would not be possible (Steppan et al. 2002). Alternatively, constraints can be considered in a 'positive' view since the evolutionary history of an organism channels it along specific pathways of evolution (Gould 1989; Schwenk 1995; Richardson and Chipman 2003), favoring those trait combinations that have more genetic variation (Steppan et al. 2002). Since many categories of constraints have been described (reviewed by Alberch 1982; Cheverud 1984; Maynard Smith et al. 1985; Antonovics and van Tienderen 1991; Schwenk 1995; Hall 1996; Raff 1996; Arthur 1997; Richardson and Chipman 2003), we will define both developmental and genetic constraints as used here before stating the rationale and objectives of our study.

Developmental constraints are defined as biases on heritable phenotypic variation, caused by properties of developmental systems (Maynard Smith et al. 1985). As recently reviewed by Richardson and Chipman (2003), several mechanisms have been grouped under this type of constraint. Using the palimpsest model as a general

framework (Hallgrímsson et al. 2007b; Hallgrímsson and Lieberman 2008), and considering that we will focus on an environmental effect exerted exclusively during the last stages of the postnatal development of the human skull (artificial cranial deformation practiced on children, see below), our definition of developmental constraint is limited to any epigenetic buffering occurring at these final phases of neurocranial growth. More precisely, we will explore how a series of mechanical strains applied to the neurocranium during brain growth provoke disruption of normal covariation patterns. Since artificial deformation is applied to newborns and infants, all previous developmental epigenetic effects occurring at early phases of prenatal development are beyond our analysis.

Genetic constraints are defined in a more straightforward way within the framework of quantitative genetics, which provides a means for predicting the outcome of phenotypic evolution, given measurable selective pressures (Lande and Arnold 1983). A complex trait will evolve either by direct selection on that trait or by the selection on all other traits correlated with it (Steppan et al. 2002). Therefore, genetic constraints can be intended as the axes of variation that are favored or restricted by the additive effect of many genes determining the expression of the phenotypic trait. These constraints can be studied after examination of the **G** matrix, the matrix of additive genetic variances and covariances among traits (Lynch and Walsh 1998). The **G** matrix summarizes the genetic basis of the traits since it is determined by the allelic frequencies in the population and by the distribution of the additive phenotypic effects on those alleles (Lande 1979; McGuigan 2006). Eigenanalysis such as principal component analysis (PCA) can decompose the **G** matrix in a set of new variables; that is, eigenvectors with associated eigenvalues, which are linear combinations of the original traits that represent vectors in phenotypic space (McGuigan 2006). The first eigenvectors (with larger eigenvalues) would correspond to those directions with more associated additive genetic variance in which evolutionary change is more likely. On the contrary, the last eigenvectors (with smaller eigenvalues) would correspond to those 'forbidden' trajectories of evolutionary change that have small or no additive genetic variation. The **G** matrix is thus a key parameter of quantitative genetics that measures the patterns of covariation defined by the epigenetic system (Cheverud 1984). In consequence, an inspection of the **G** matrix for human craniofacial shape could bring some clues regarding to what extent neurocranial globularity is constrained as a whole.

Here we apply two separate approaches to investigate constraints on neurocranial globularity, one developmental, the other genetic. First, we analyze a composite sample of normal, non-deformed (ND) skulls versus artificially deformed ones in order to detect which aspects of normal morphological integration are conserved or else altered during the postnatal growth of the deformed individual. Since artificial deformation is a pure environmental effect, this approach could indicate how a skull experiencing brain growth reacts against the application of a given deformation device. Second, we will use the **G** matrix for skull shape of a modern human population to simulate the response to selection to deformation of the neurocranial structures in particular, and the whole skull in general, in order to detect favored or avoided directions (constraints) of shape change.

Developmental Constraints: Morphological Integration in Deformed Skulls

Artificial cranial deformation (ACD) was ubiquitous among many modern human populations, and particularly frequent among pre-contact New World groups (Dembo and Imbelloni 1938). Some authors have interestingly noted that deformed skulls provide a 'natural experiment' (Antón1989; Antón et al. 1992; Cheverud et al. 1992; Kohn et al. 1993; Antón and Weinstein 1999) that enables the study of morphological integration patterns and its putative disruption effect. This is due to the mechanical strains experienced during the application of the deformation device, which are concomitant with the epigenetic effect of the growing brain as a primary driver of cranial vault development (Jiang et al. 2002). More particularly, each ACD type can be considered as a biomechanical experiment in which a particular set of forces are applied to the neurocranium of some members of a given population at early stages of postnatal development. Thus, the localization of the environmental stimuli is to some extent controlled by the cultural practice itself, whereas the genetic differences are limited to within-population variability. In a previous paper, we have suggested that matrices of phenotypic variance/covariance are rather stable across modern human populations (González-José et al. 2004b). Thus, variation on ACD practices across groups, as well as variation of ACD intensity across individuals, brings an unusual opportunity to track disruptions of this observed stable pattern of morphological integration.

Many particularities concerning the nature and practice of ACD allow us to examine morphological integration after a set of a priori and a posteriori hypotheses. First, it is important to remark that there is certain regularity on the practice of ACD across several periods and regions (Dembo and Imbelloni 1938). In general terms, three main types of deformation are observable across the New Word: annular (A), lambdoid flattening (LF), and fronto-occipital (FO). Annular deformation is achieved by circumferentially, tightly wrapping the head with a binding that is

progressively adjusted around the cranial vault as the child grows up. Conversely, LF and FO modifications result from the application of a cradleboard or a headdress on the lambda region or on the frontal and occipital regions of the cranial vault, respectively. Note that this general classification is also used by several authors (Antón 1989; Antón et al. 1992; Cheverud et al. 1992; Kohn et al. 1993; Antón and Weinstein 1999).

Second, the three main types of deformation greatly differ in its biomechanical nature. For instance, the annular deformation affects both the cranial base and the vault, restricting the medial-lateral growth of the cranial vault and resulting in longer and narrower crania (Fig. 1). Conversely, the effects of LF are focused in the posterior part of the vault, around the lambda region. In this case, posterior growth of the cranial vault is restricted, resulting in shorter and wider crania. FO deformation is similar to LF, but an additional strain is focused on the frontal bone, around the metopion, restricting the anterior–posterior growth. Previous studies by Antón (1989, 1994) have shown that the face and cranial base adjust to vault deformation according to the type of deformation. LF and FO faces are short and wide, whereas A faces are narrow and more projecting. Moreover, analyses made on annular and occipital flattening of different Amerindian populations (Kohn et al. 1993, 1995) suggest that the response of the cranial base and face to the deformation stimuli is variable depending on the ACD type.

Finally, deformation devices were applied during the early stages of the growing skull. Since the cranial base, the vault and the face differ in its growth and developmental timing, it is expected that deformation will have a greater impact on those regions that are still under development (Bastir et al. 2007).

All of the above considerations should be considered in the light of craniofacial development. Taking into account the biomechanical implications, distribution, and timing of ACD in combination with the effect of brain growth as a source of covariation of neurocranial structures, in this study we examined if morphological integration patterns are conserved or else disrupted in deformed skulls. More particularly, we compared the patterns of morphological integration of each type of deformation and tested if there are any significant differences between them, assessing if there is some trait combination whose morphological integration is reinforced and thus stronger in deformed crania. Moreover, we assessed if perturbation of the normal pattern of integration is related to the biomechanical particularities of each deformation practice.

In order to address these questions we will examine the following two hypotheses. Firstly, Hn1 assumes that brain growth is the main developmental process that configures covariation patterns on the vault and base, and states that there are some key morphological aspects influencing the skull that are always conserved, either in the deformed or the ND sample. Such a result would be expected if brain growth is a mechanism strong enough in order to enable the conservation of some covariation pattern even in extremely deformed skulls. The lack of some integration pattern observable across different ACD types entails rejection of this hypothesis. Non-rejection of this hypothesis points towards an important role of brain growth as a source of covariation patterns. Secondly, Hn2 expects that disruption of the normal integration pattern is more likely in ACD types produced by localized and intense strains of deformation, such as the LF practice. The alternative expects that the degree of covariation will decrease in those ACD types whose impact is more subtle and spread across several cranial structures, as the annular deformation type.

Genetic Constraints: Morphological Integration and Response to Selection

As explained above, artificial deformation involves plastic changes in skull shape by restricting brain and bone growth in certain directions and causing typical dysmorphologies. Although this is certainly not a genetic change, it might be interesting to explore how the entire developmental program of the skull would respond to such deforming forces if they were induced by directional selection. If this was the case, the entire set of epigenetic program subsumed in G would certainly play a role in determining the response of

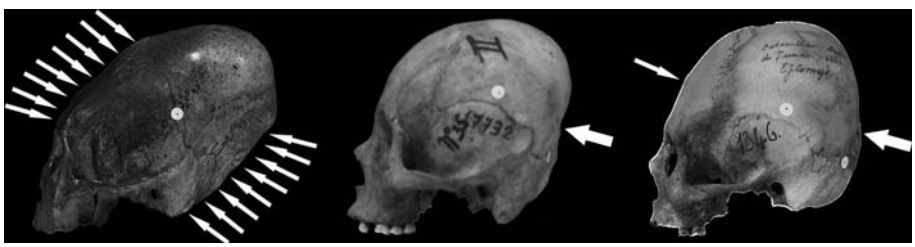

Fig. 1 Lateral view of skulls showing annular (A, *left*), lambdoid flattening (LF, *center*), and fronto-occipital (FO, *right*) deformation practices. Arrows indicate compression strains exerted during the deformation. Note that compression on the basicranium is only exerted on the annular case

selection and the skull shape of the next generations (Lynch and Walsh 1998). By exploring this issue, we can compare the effects of developmental and genetic constrains on neurocranial globularity and skull shape and assess if they produce similar outcomes.

To inspect the genetic constraints one must have previous knowledge of the genetic covariance matrix for skull shape (Lynch and Walsh 1998). In humans, it is difficult to obtain this key quantitative genetic parameter since large collections of skulls with known genealogical relationships are almost non-existent. For instance, we do not have any genetic data on our American samples of deformed and ND skulls, but we can test the previous hypotheses using the **G** matrix for skull shape estimated from another sample of modern humans coming from Hallstatt (Austria) (Martínez-Abadías 2007). As far as we are concerned, this might be a good proxy to the genetic architecture of the shape of the human skull.

Studies of the **G** matrix evolving *in silico* have lead to testable hypotheses about the relative effects of different parameters, and the effects of variable parameter values (McGuigan 2006). Simulations *in silico* of the evolutionary behaviour of the **G** matrix can be done using the multivariate breeder's equation (Lande and Arnold 1983), which provides a means for predicting the evolution of complex traits if information about directional selection and the degree of resemblance among relatives is available (Lynch and Walsh 1998). Specifically, we will use this methodology to test a third hypothesis. Hn3 considers that neurocranial globularity is genetically constrained and that deformations of the cranial vault will be buffered through pervasive genetic correlation between cranial regions. This would be expected if the effects of deformation forces (represented by the simulated selection gradients), and therefore the departures from normal patterns of neurocranial globularity (represented by the total responses to selection), were reduced by means of genetic integration. This will be tested using two simulations: the simulation of a localized deformation, such as LF, and the simulation of a generalized deformation, such as annular deformation. This hypothesis is rejected if either of the simulations of artificial deformation (the localized or the generalized one) produce a response to selection in which neurocranial globularity is not conserved; that is, if the simulated deformation forces produce strong and localized shape changes and disrupt neurocranial globularity as compared to normal patterns of morphological integration in ND skulls.

Materials and Methods

Developmental Constraints: Morphological Integration in Deformed and Non-Deformed Skulls

We analyzed 229 adult skulls from five recent, pre-contact Amerindian populations, which present varying levels of ACD. Sample composition and further details are provided in Table 1. Previous studies concerning population genetics and dynamics of these populations can be found in Sciulli (1998, 2001), Luis et al. (1999), Tatarek and Sciulli (2000), González-José (2003), González-José et al. (2002, 2004a, 2005), Sardi and Pucciarelli (2001), and Paschetta et al. (2008).

Sex and age were estimated following diagnostic traits provided by Buikstra and Ubelaker (1994). After digitizing, each skull was assigned to a type of deformation by visual classification. Skulls were assigned to the following categories: ND, A, LF or FO. In addition, within each deformation category (A, LF, FO) each skull was classified according to the intensity of the deformation with a scale ranging from 0 (mild) to 2 (severe).

Measurements and Landmark Coordinates

Three-dimensional landmark coordinates were collected using a Microscribe G2X digitizer, which has a reported accuracy of 0.23 mm and a measured error of 0.03 mm.

Table 1 Developmental constraints analysis: sample composition

Sample	Geographic origin	Non-deformed (ND)		Annular (A)		Lambdoid flattening (LF)		Fronto-occipital (FO)		Total
		F	M	F	M	F	M	F	M	
Araucano	Central Argentina	23	16			9	14			62
Bolivians	Southern Bolivia	5	12	13	11		2	4	3	50
Woodland and late prehistoric	Ohio Valley (USA)	6	8			7	7		1	29
Pampa Grande	Northwestern Argentina	14	9			5	15			43
Río Negro	Northeastern Patagonia (Argentina)	9	9	7	8	2	8	1	1	45
Total (sex)		57	54	20	19	23	46	5	5	
Total (ACD types)		111		39		69		10		229

Each individual is represented by 32 homologous landmarks that were assigned into different subconfigurations of 7 basicranial, 15 facial and 10 vault landmarks (Fig. S1). Size and shape were captured in two different ways: using geometric morphometric and traditional morphometric methods. First, the original basal, facial, and vault configurations were separately superimposed using a Generalized Procrustes Analysis in order to remove the effects of translation, rotation, and scaling (Rohlf and Slice 1990). The Procrustes superimposition removes the scale but not the allometric shape variation that is related to size. To remove correlations among shape variables due to allometry, we computed the residuals of the regional Procrustes coordinates on centroid size and standardized each dataset by its mean centroid size using IMP-ThreeDStand6 (Sheets 2004). Landmark coordinates superimposed and free of allometry were used as the input data for three different analyses: partial least squares (PLS), ANOVA, and partial correlation analysis. The last two tests were performed upon the principal components (PCs) of the aligned data.

Besides this morpho-geometric approach, classical measurements were also obtained from the raw landmark coordinates in order to represent dimensions that are hypothesized to be determinants of craniofacial shape (Enlow 1990; Lieberman et al. 2000; Hallgrímsson et al. 2007a, b). Following Hallgrímsson et al. (2007a), we obtained the maximum width, length, and centroid size of each region, as well as the sphericity of the braincase (Table S1). Sphericity is computed as the variance of the distance of the neurocranial landmarks to the centroid. Linear distances were log-transformed in order to equalize the dimensionality of all variables and to uncouple the variances from the means. Sphericity is a dimensionless variable, and as such it was not transformed. The definitions of each measurement are provided in Table S1. To remove correlations between these variables due to cranial size, we regressed all variables (except the sphericity) on the centroid size of the respective structure. All of the subsequent analysis were entirely performed on the residuals of those regressions.

Statistical Analyses

Patterns of covariation between two (and potentially more) blocks of variables can be explored by means of PLS. PLS can be used to study covariation between two blocks of shape variables, making it potentially useful for studies of morphological integration (e.g. Bookstein et al. 2003; Bastir 2004; Bastir et al. 2004; Zelditch et al. 2004). Here, the patterns of morphological integration among the cranial vault, the basal, and the facial configurations were analyzed using the method of singular warps (Bookstein et al. 2003). Singular warps are a special case of PLS (cf. Rohlf and Corti 2000; Bookstein et al. 2003; Gunz and Harvati 2007) used to quantify and visualize the covariation of anatomical regions when all variable blocks are shape coordinates. Blocks of landmarks are defined a priori; afterwards, the linear combinations of the original shape variables that provide the best mutual cross-prediction between these blocks of landmarks are computed. We used the IMP-PLS3D software (Sheets 2005) to estimate the amount of covariance explained by the paired singular vectors (the SVD axes) and the correlation ''r'' of the scores of the specimens along the singular axes of the two blocks. The correlation coefficient ''r'' can be used as a measurement of integration between two blocks of shape variables (Klingenberg et al. 2001; Bookstein et al. 2003; Bastir and Rosas 2005). To assess the statistical significance of the singular warp scores as well as of their correlations, we performed permutation tests ($N = 10{,}000$). The IMP_PLS3D software only allows the comparison of two sets of shape data. Therefore, three different PLS-analyses were performed, and three correlation coefficients were compared: r-VB quantifies the integration between the vault and the base; r-VF quantifies the integration between the vault and the face; and r-BF quantifies the integration between the base and the face. Correlations were obtained for the whole sample and for each type of deformation.

Although there is no formal statistical test to detect differences among r-VB, r-VF, and r-BF on deformed and ND sub-samples, Hn1 will not be rejected if at least one significant singular vector is found across the whole composite sample. This would suggest that there is at least a single axis of covariation underlying deformed and ND skulls. Furthermore, greater similarity among the ND skulls and those types of deformation caused by localized strains (such as LF) would be consistent with Hn2.

The fitted coordinate configurations of the specimens were analyzed using PCA. In order to transform landmark coordinates into shape variables, we computed the PCs of each landmark configuration; that is, separately for the cranial vault, the base and the face. In order to detect which aspects of skull size and shape are more influenced by the deformation practices, the raw classical measurements and the PCs explaining more than 60% of variation were compared among types of deformation, populations, and sexes using ANOVA with Bonferroni's correction for multiple comparisons.

Partial correlation is a procedure that determines the correlation between any two variables if the remaining ones were held constant. Here we examined the patterns of covariation among classical measurements and PCs by correlation and partial correlation analyses (Hallgrímsson et al. 2007a). The first null hypothesis (Hn1) predicts that at

least one pair of traits will covary significantly across the different ACD subsamples. Alternatively, Hn2 predicts that ND skulls will share more significant partial correlations with ACD types shaped by localized changes (LF) than with ACD types involving global strains (A).

Genetic Constraints: Morphological Integration and Response to Selection

To estimate the **G** matrix for skull shape and to assess the genetic constraints of neurocranial globularity, we analyzed a sample of 390 complete crania from the ossuary of Hallstatt (Austria), which provides a large collection of human skulls with associated genealogical data. This material has been accumulating since the eighteenth century until recently as a result of a local tradition: skeletal remains were recovered from the Catholic churchyard when requested from their descendants and the crania were decorated with paintings and stored at the charnel-house. Skulls can be individually identified thanks to their decorations, which usually include the names of the individuals. Parish records permit to reconstruct genealogical relationships, making it possible to estimate directly the **G** matrix for skull shape.

The sampled individuals were mainly adults (91%) from both sexes (41% females, 59% males), and a small proportion of the skulls showed slight dysmorphologies (12%). To reconstruct the genealogies of the Hallstatt population we compiled the complete records of births, marriages and deaths from 1602 to 1900, which included 18,134 individuals. From the analyzed skulls, 350 fall into the extended and multigenerational genealogies. A more detailed description of this sample can be found elsewhere (Sjøvold 1984, 1995; Martínez-Abadías 2007).

Sexing, aging and landmark digitizing were performed using the same procedures as explained above. In this analysis, we characterized skull shape using a hemicranial configuration of 29 anatomical landmarks distributed over the left side of the entire skull (Fig. S2).

Quantitative Genetic Analyses

According to standard approaches to quantitative genetics, the phenotypic variation of a trait (V_P) can be decomposed into its components of genetic (V_G) and environmental (V_E) variation by the expression $V_P = V_G + V_E$ (for a review see Falconer and MacKay 1996; Lynch and Walsh 1998). This decomposition relies on the phenotypic resemblance between relatives and it is possible provided there is associated genetic or demographic data. The phenotypic variation is thus obtained from the direct measurement of the trait; the additive genetic variation is estimated as the phenotypic covariation between relatives; and finally, all the variation that can not be explained by familiar relationship is considered as residual, environmental variation.

To estimate the phenotypic, genetic and environmental components of variation of skull shape we combined multivariate methods of geometric morphometrics and quantitative genetics following Klingenberg and Leamy (2001). This approach enables to preserve the multivariate nature of shape and to detect complex patterns of shape change (Klingenberg and Monteiro 2005). Skull shape is thus treated as a whole and is not dissected in multiple distance and angular measurements, preserving the anatomical relationships between the different structures and regions that made up the skull and accounting for the covariation patterns among them.

Following geometric morphometric approaches and using the MorphoJ software package (Klingenberg 2008), we first performed a Procrustes superimposition on the raw landmark data (Fig. S2) to estimate the phenotypic variation of human's skull shape. Then we computed a PCA from the Procrustes fitted coordinates in order to reduce the dimensionality of the data. The resultant PCs were used as the phenotypic input data for the quantitative genetic analysis.

To break down the phenotypic variation (**P**) into its components of additive genetic (**G**) and environmental (**E**) variation we used a restricted maximum likelihood method (REML), as implemented by the software package VCE5 (Kovac and Groeneveld 2003). In comparison to other quantitative genetic methods (e.g. parent-offspring regression or sib analyses), REML analytical methods are advantageous because they incorporate multigenerational information from unbalanced datasets. Moreover, they are not limited by assumptions of non-assortative mating, inbreeding or selection (Kruuk 2004).

REML methods are based on the so-called 'animal model', which follows a mixed linear model that jointly accounts for fixed and random effects to describe each individual's phenotype (Kruuk 2004). We defined a multivariate model that included the first 32 shape PCs (accounting for 89.6% of the total phenotypic shape variation) as random dependent variables, skull centroid size as a covariate, and individual's sex, age and deformation status as fixed effects. REML methods estimate the components of variance (**G, P** and **E**) using an iterative procedure that maximizes the likelihood of observing the actual data (Lynch and Walsh 1998).

To perform the response to selection analyses, the **G** and **P** covariance matrices computed by VCE5 were imported to MorphoJ (Klingenberg 2008) and converted back to the space of the original landmark coordinates from the coordinate system of PC scores (Klingenberg and Leamy 2001). These quantitative genetic analyses are based on the

multivariate breeder's equation (Lande 1979; Lande and Arnold 1983)

$$\Delta\mu = \mathbf{G}\mathbf{P}^{-1}\mathbf{s} = \mathbf{G}\beta$$

where $\boldsymbol{\Delta\mu}$ is the response to selection; **G** is the additive genetic covariance matrix; **P** is the phenotypic covariance matrix; **s** is the selection differential; and $\boldsymbol{\beta}$ is the selection gradient.

The selection response $\boldsymbol{\Delta\mu}$ is a vector that reflects the shape change between the phenotypic trait mean after and before the selection episode. It is estimated as the vector of differences between the mean shapes of the parental and offspring generations (Klingenberg and Monteiro 2005). The selection differential **s** specifies the intensity of selection, and under directional selection it is computed as the vector of differences between the shape means in the parental generation before and after selection. It also can be considered as the vector of covariances between the shape variables and relative fitness. The selection gradient $\boldsymbol{\beta}$ is also a measure of the strength of selection that can be interpreted as the vector of regression coefficients from a regression of relative fitness. Together with estimates of **G** and **P**, either of these can be used as selection vectors to estimate the response to selection (Klingenberg and Monteiro 2005).

To represent the magnitude and direction of selection, we used an auxiliary shape variable proportional to the selection gradient instead of the selection differential (Klingenberg and Leamy 2001). This alternative analyzes direct selection rather than total selection (Lande and Arnold 1983), and thus disregards correlated selection. Because $\boldsymbol{\beta}$ is not a vector in shape space (Klingenberg and Monteiro 2005), the use of a scaled version of the selection gradient **a** makes it possible to visualize the shape changes associated to the selection gradients. The auxiliary shape variable is computed as $\mathbf{a} = \boldsymbol{\beta}(\boldsymbol{\beta}^{\mathrm{T}}\boldsymbol{\beta})^{-0.5}$, has the same direction as $\boldsymbol{\beta}$, and is related to it by a proportionality constant **c**, so that $\boldsymbol{\beta} = c\mathbf{a}$.

Furthermore, as suggested by Klingenberg and Leamy (2001), we modified the standard formula of the multivariate breeder's equation to be used after geometric morphometric data. As the **P** matrix was computed from the first 32 PCs and therefore was singular when converted back to the coordinate system of the landmark coordinates, we used the Moore-Penrose generalized inverse $\mathbf{P}^{-}$ instead of $\mathbf{P}^{-1}$ in the computations (Klingenberg and Leamy 2001).

From the multivariate breeder's equation (Lande 1979; Lande and Arnold 1983) it is straightforward that the evolution of a given trait is not only a function of the additive genetic variance and selection on that trait, but also of the genetic variance of other traits with which it covaries genetically (Lande and Arnold 1983). Therefore, the covariation patterns between traits reflected in **G** can be considered as genetic constraints because they will deflect the response vector $\boldsymbol{\Delta\mu}$ from the originally selected direction of change imposed by the selection gradient $\boldsymbol{\beta}$ (Steppan et al. 2002).

We applied this quantitative genetic model for evolutionary response to explore how neurocranial globularity would respond to putative selective events altering the normal morphological patterns. To do this we defined two selection gradients ($\boldsymbol{\beta}$), each one simulating the morphological effects produced by two different deformation practices: a localized one, such as LF deformation, and a generalized one, such as A deformation. Then, to test if such departures are genetically constrained (Hn3), we estimated the hypothetical response to selection applying the multivariate breeder's equation.

The selection gradients were constructed using a graphical user interface in MorphJ (Klingenberg 2008), which enables the user to drag the landmark points of the mean shape configuration to specify a shape change. The landmark coordinates of the consensus skull shape of the Hallstatt population were modified to produce a configuration of shape that reflected the selective regime required to produce the skull shape associated with each of the deformation practices. The first simulation concerned the LF deformation. As this practice locally restricts cranial growth at the posterior region of the neurocranium, we simulated it by a forward shift of lambda. The second simulation concerned the annular deformation, which is the most generalized and complex deformation practice because it affects the whole braincase. To represent it in a simplified way, we simulated the main biomechanical strains of this type of deformation by a backward shift of metopion, a forward shift of lambda, an upward shift of bregma and lateral shift of euryon towards the sagittal plane. This represents an anterior–posterior and a lateral compression, and forces the braincase to grow towards a dorsal direction.

For each simulation, the specified landmark shifts representing $\boldsymbol{\beta}$ were projected onto the tangent space to shape space (Dryden and Mardia 1998) to ensure that the selection gradient was in the same space as the variation characterized by the **G** and **P** matrices. This can result in smaller shifts of other landmarks to compensate for changes in overall position, orientation and size. To make shape changes visible, we magnified the magnitude of selection gradients to ten standard deviations of relative fitness per standard deviation of the respective shape variable.

Finally, as the predicted selection response $\Delta\boldsymbol{\mu}$ is usually in a different direction from the direction of selection that was entered into the analysis, we decomposed this total response into components of direct and correlated response to selection following Klingenberg and Leamy (2001). The direct response is a scaled version of the selection gradient

and these two vectors are in the same direction in shape space; whereas the correlated response is a vector perpendicular to the direct response. All the magnitudes of the responses to selection are measured in Procrustes distance units.

Results

Developmental Constraints: Deformed Versus Non-Deformed Skulls

Partial least squares analysis provides independent descriptions of the cranial vault, the facial, and the basal configurations, as well as estimations of the covariation among these three blocks. The relationships between the first singular warps of each configuration are plotted as singular warp scores in Fig. 2. Singular warps analyses show strong patterns of morphological integration. The interaction among the cranial vault and the base is stronger (Fig. 2a, 48% of covariance explained by the first singular warp) than that among the vault and the face (Fig. 2b, 25% of covariance explained) as well as than that among the base and the face (Fig. 2c, 29% of covariance explained).

Regarding the behavior of ACD types, in the comparisons vault-base and vault-face (Figs. 2a, b), the scores from the first dimension clearly separate LF (negative values) from annular deformed skulls (positive values). The opposite position is obtained in the base-face test (Fig. 2c). Besides the direction and magnitude of the axes of ND covariation displayed by these types, there is still a single linear trend in the covariation between blocks. Note that in the case of the vault-base comparison (Fig. 2a) the amount of variance explained in one block due to variations in the other one accounts for 48% of the total variation. Moreover, there are remarkable differences among the linear fit corresponding to each type of deformation (see below).

The polygons of deformation depicting shape changes from negative to positive values across the first singular vectors are provided in Fig. 3. The vault-base comparison shows that the first singular warp represents the shape difference of individuals with long and narrow vaults and less flexed and narrow bases versus skulls with short and wide crania and more flexed and wider bases (Fig. 3a). In the vault-face comparison, the same variation in vault corresponds to narrow and tall faces versus wide and low faces (Fig. 3b). Finally, in the base-face comparison, short and wide bases are related to wide and low faces, versus long and narrow bases concomitant with high and narrow faces (Fig. 3c).

The correlations "r" of the scores of specimens along the singular axes of each pair of blocks, computed independently for each ACD type, are shown in Fig. 4. They indicate that the stronger pattern of integration among the vault and the base is also maintained in the LF subsample, but disrupted in the annular and the FO ones. Unfortunately, to the best of our knowledge there is no released software available to perform a permutation test of differences among the correlation coefficients of singular values obtained after three-dimensional data. However, the PLS results suggest some degree of disruption of covariation patterns among the ACD types.

The three-way ANOVA (considering population, sex and ACD type as covariates) shows that most classical measurements and almost all PCs significantly differ among populations (Table 2). Only two low-order PCs related to the shape of the cranial vault and the base, as well as facial size, vault width and base length differed between sexes after Bonferroni adjustment for multiple comparisons. Regarding ACD types, all higher-order vault and base PCs, as well as all classical measurements (excepting facial length) vary significantly among types of deformation (Table 2).

Classical measurements and the first three PCs describing shape variation on each module were used to compute the matrix of partial correlations among traits separately for each ACD type (Fig. 5). Because of its low sample-size, the FO series was not included in this analysis. Mantel tests reveal that the matrices of partial correlations among traits computed on the different ACD types are significantly correlated ($P < 0.00000$ after 10000 permutations). However, observation of the within-ACD type pattern of integration reveals further patterns. For instance, it is informative about covariation patterns that are conserved among types; evidences which traits are covarying stronger within a given type; and shows which covariation patterns are disrupted or weakened among deformed skulls. The partial correlations that are significant on the three subsamples (ND, A, LF) suggest that there is a pattern of morphological integration conserved in deformed and ND series. This pattern is dominated by associations among basal size and width, basal shape and length, and vault size and length. Furthermore, the significant correlation between sphericity and vault width and size is conserved both in the ND and the LF series. Low correlations involving facial size and shape variables reflect that the face varies more independently than the vault and the base. Interestingly, integration among facial shape and length increase in the deformed series in comparison to the ND one, but this could be considered as a by-product of the decreased integration between the vault and the base in the deformed skulls.

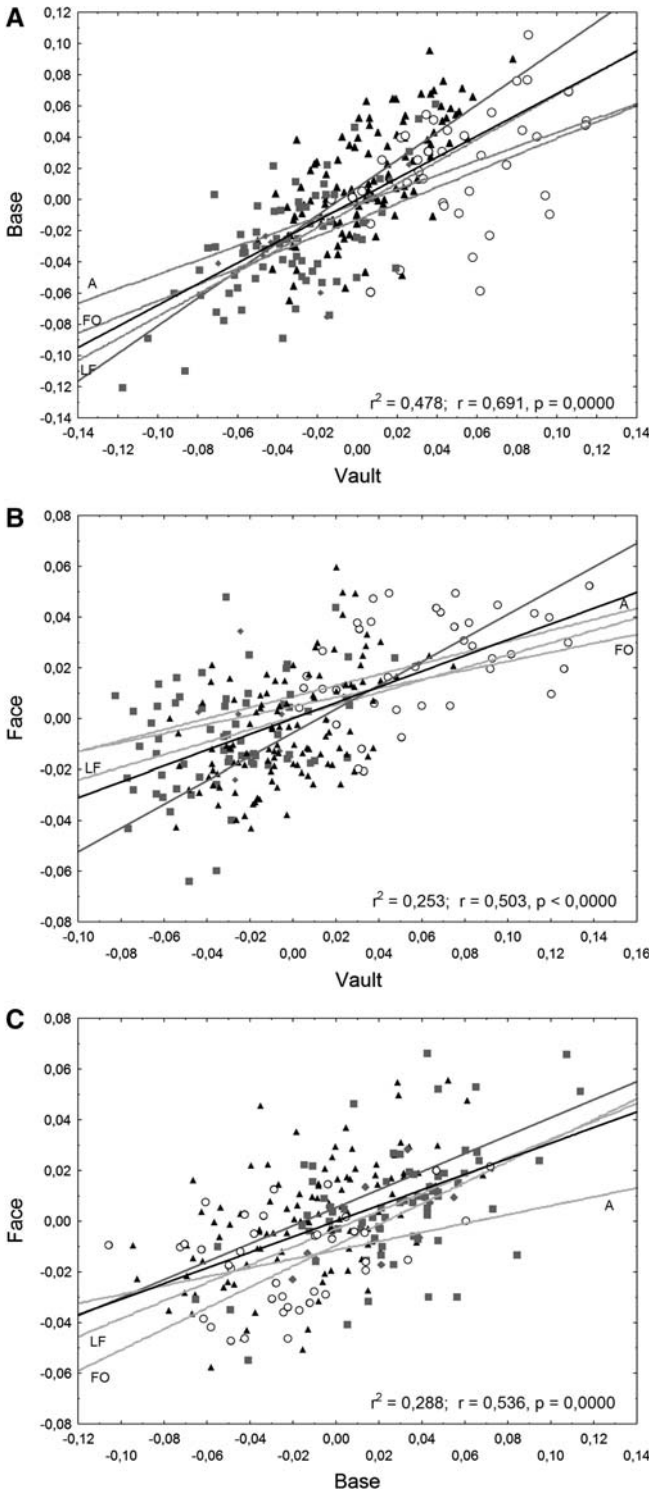

Fig. 2 First singular warp scores for the set of all deformed and non-deformed skulls. **a** vault-base, **b** vault-face, **c** base-face. *Black solid triangles*: non-deformed; *open circles*: annular deformation; *grey squares*: lambdoid flattening; *grey diamonds*: fronto-occipital deformation. Lines represent the best linear fit for each ACD type scatterplot independently. *Black solid line*: linear fit for the whole sample; *grey solid line*: non-deformed skulls; *grey dotted line*: A, LF, and FO deformation types. The parametric correlation (r), the variance explained (r^2), and the *P*-value (*P*) of the correlation among scores corresponding to the two blocks are provided in the *right-bottom* corner

Genetic Constraints: Responses to Hypothetical Selection

Concerning the simulation of LF (Fig. 6), which is a localized deformation practice, results showed that the total response to selection (whose magnitude was of 0.077 units of Procrustes distance) included shape changes distributed throughout the skull, but especially in the cranial vault. These shape changes involve an anterior–posterior compression of the braincase (lambda, opisthocranion, inion and opisthion shift forward whereas metopion, bregma and vertex shift backward) accompanied by a lateral expansion of the whole skull and an inferior shift of the landmarks delimiting the alveolar region. This total response consists

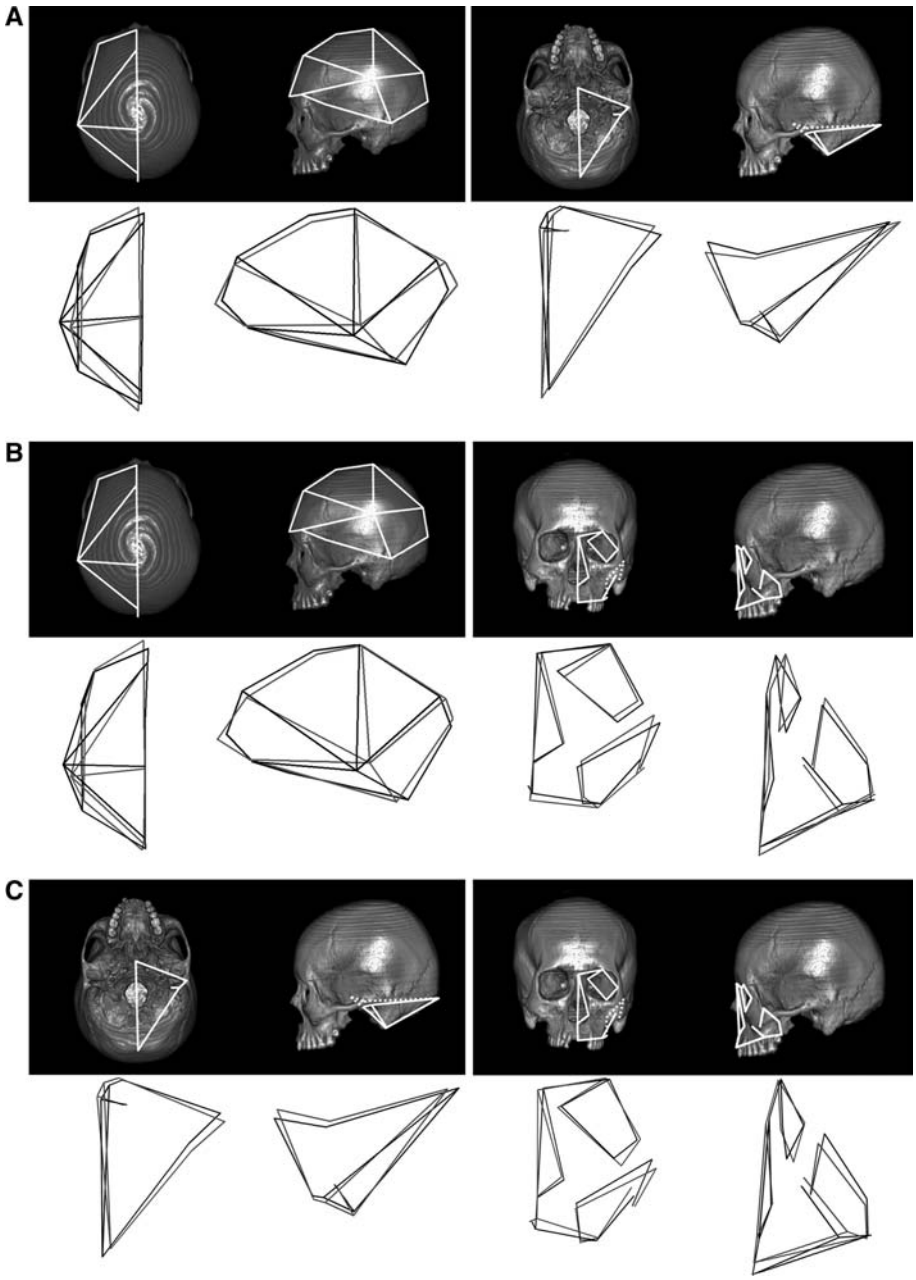

Fig. 3 First singular warp for the subset of all deformed and non-deformed specimens shown as polygons for each block on the following comparisons: **a** vault-base, **b** vault-face, **c** base-face. *Grey wireframe*: deformation towards the positive values; *black wireframe*: deformation towards the negative values

of a direct response that is localized to the lambda and a correlated response affecting mostly the landmarks of the cranial vault. The magnitude of the correlated response (0.067) exceeds that of the direct response (0.039), indicating that the direction of response has been deflected substantially from the direction of the selection gradient by an angle of 59.8°. This indicates that shape changes in the total response to selection are mainly due to genetic covariation patterns between traits, which are expressed in the **G** matrix and may be considered as genetic constraints.

The simulation of the annular deformation (Fig. 7), which is a more generalized deformation practice, provided a total response to selection (0.079 units of Procrustes distance) that showed even more pervasive shape changes affecting the cranial vault, the base and the face. There is a substantial anterior–posterior compression of the cranial vault, a posterior shift of the basal landmarks (hormion, basion and opisthion) and a forward and inferior shift of the facial landmarks. The direct response is a scaled version of the selection gradient and the correlated response mainly shows the shape changes described for the total response to selection. This is because the main component of the total response is the correlated response, and its magnitude (0.068) exceeds that of the direct response (0.040). Thus, the total response is deviated from the direction of change of the selection gradient by the high strength of the

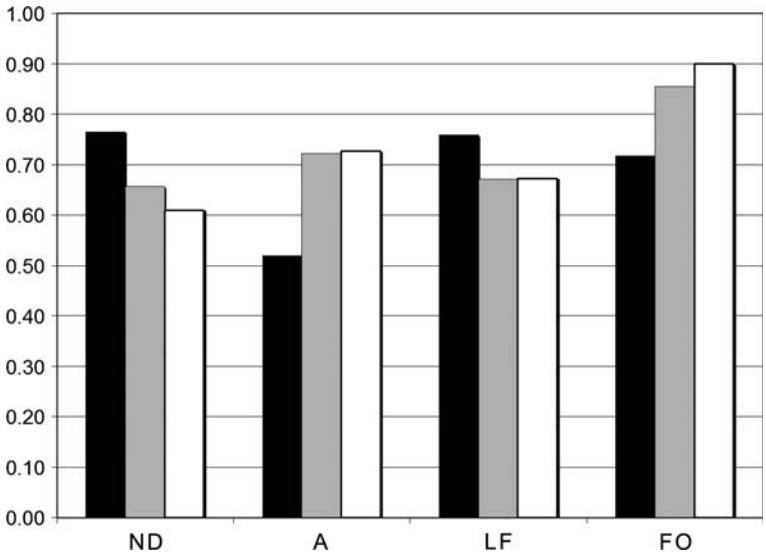

Fig. 4 Correlation coefficients of singular warp (SW) scores. *Black columns*: SW1 correlations among vault and base; *grey columns*: SW1 correlations among vault and face; *white columns*: SW1 correlations among base and face. ND: non-deformed, A: annular, LF: lambdoid flattening, FO: fronto-occipital

correlated response (59.5°). Overall, the results obtained from both simulations show that the total response to selection includes shape changes that mainly maintain neurocranial globularity through similar integration patterns.

In summary, this study evidences that neurocranial globularity is a highly constrained trait. Analyses of morphological integration performed on the sample of deformed and ND skulls showed that developmental constraints preserve some aspects of normal morphological integration even in the most deformed skulls. Moreover, quantitative genetic analyses simulating the hypothetical potential responses to selection to neurocranial shape changes similar to the real case of artificial deformation showed that the **G** matrix for skull shape integrates neurocranial globularity at the genetic level. Therefore, our results suggest that neurocranial globularity is constrained both at the phenotypic and the genetic level.

Discussion

A constraint is a mechanism that restricts or biases the potential for evolutionary change (Cheverud 1984). In consequence, constraints are forces opposing the evolution in at least some directions of change or else favoring and channeling the evolution in other directions of the phenotypic space (Maynard Smith et al. 1985; Klingenberg 2005). These constraints are closely linked to morphological integration patterns, because it is covariation between traits that limits change in some directions and makes certain combinations of traits difficult to achieve (Klingenberg 2005; Marroig and Cheverud 2005).

Morphological integration is defined, in a broad sense, as the connections or relationships among morphological elements (Olson and Miller 1958; Cheverud 1996; Bolker 2000; Pigliucci and Preston 2004). Morphological integration represents a constraint to evolution (Maynard Smith et al. 1985), in the sense that there are phenotypes (that is, trait combinations) that cannot evolve in the population because they lack genetic variation (Lynch and Walsh 1998; Merilä and Björklund 2004). This is because traits often share some of their genetic basis, and the additive genetic covariation among traits prevents them from evolving independently (see Mc Guigan 2006 for a review on this topic).

On the other hand, morphological integration ensures the maintenance of the function and development of complex phenotypes. As a general rule, large amounts of genetic variation are constrained through a limited set of developmental processes. Recently, Hallgrímsson et al. (2007b) and Hallgrímsson and Lieberman (2008) have proposed that the overlaying of mechanisms participating in the development (e.g. neural crest migration, patterning and proliferation, facial process fusion, cell condensation and differentiation, cartilage growth, brain growth, muscle–bone interactions, somatic growth, etc.) determine the covariation structure of an adult skull. Without the coordination of these multiple mechanisms of integration, complex structures like a skull would not grow and function correctly (Hallgrímsson et al. 2007a).

Developmental Constraints

Artificial cranial deformation can be used as a natural experiment to analyze alterations of the human skull development. However, most ACD effects occur after birth, well after most genetic effects and many developmental processes have occurred. In this context, inspection of the neurocranial integration patterns in a sample of

Table 2 Three-way ANOVA results for comparisons of classical measurements and PCs by population, sex and ACD types

	Population		Sex		ACD type	
	F	*P*-value	F	*P*-value	F	*P*-value
Face-PC1	**11.48**	**0.0000**	7.17	0.0080	1.01	0.3882
Face-PC2	**7.47**	**0.0000**	0.43	0.5142	1.60	0.1910
Face-PC3	**8.30**	**0.0000**	0.64	0.4235	2.07	0.1049
Face-PC4	2.63	0.0245	1.59	0.2088	0.87	0.4558
Face-PC5	**7.93**	**0.0000**	1.92	0.1669	0.38	0.7642
Vault-PC1	**5.52**	**0.0001**	0.09	0.7685	**30.89**	**0.0000**
Vault-PC2	**4.71**	**0.0004**	0.20	0.6571	**6.22**	**0.0005**
Vault-PC3	2.24	0.0514	**15.38**	**0.0001**	**20.48**	**0.0000**
Vault-PC4	**11.75**	**0.0000**	0.11	0.7460	0.13	0.9398
Vault-PC5	**5.34**	**0.0001**	0.05	0.8203	**5.55**	**0.0011**
Base-PC1	**10.90**	**0.0000**	0.41	0.5215	**20.79**	**0.0000**
Base-PC2	**6.38**	**0.0000**	6.23	0.0133	**5.01**	**0.0022**
Base-PC3	**5.48**	**0.0001**	**41.50**	**0.0000**	1.73	0.1618
Base-PC4	3.18	0.0087	3.66	0.0571	0.27	0.8440
Base-PC5	**6.88**	**0.0000**	0.02	0.8815	1.54	0.2045
Sphericity	**12.09**	**0.0000**	0.11	0.7429	**42.00**	**0.0000**
Rel. Log Face cs	2.33	0.0435	**33.18**	**0.0000**	**13.22**	**0.0000**
Rel. Log Vault cs	1.75	0.1244	4.17	0.0424	**14.61**	**0.0000**
Rel.Log Base cs	**5.19**	**0.0002**	5.63	0.0185	**9.48**	**0.0000**
Rel. Log Vault W	3.57	0.0040	**26.31**	**0.0000**	**43.76**	**0.0000**
Rel. Log Face W	1.53	0.1811	4.01	0.0464	**8.60**	**0.0000**
Rel. Log Base W	**5.20**	**0.0002**	5.63	0.0185	**9.47**	**0.0000**
Rel. Log Vault L	2.40	0.0381	9.27	0.0026	**45.88**	**0.0000**
Rel. Log Face L	2.15	0.0604	0.30	0.5858	2.97	0.0329
Rel. Log Base L	3.40	0.0055	**14.67**	**0.0002**	**22.09**	**0.0000**

Bolded values are significant at $\alpha = 0.05$ after Bonferroni's adjustment for 25 comparisons

W width, *L* Length, *cs* centroid size, *Rel* relative

individuals whose crania were artificially deformed and the comparison with the integration patterns of ND individuals can help to identify potential epigenetic developmental constraints on neurocranial globularity occurring exclusively on the last phases of postnatal development. In this context, results obtained on our sample of postnatal-deformed skulls may reflect the influence of the growing brain as one of the main factors driving covariation patterns among the cranial vault (Jiang et al. 2002) and, to a lesser extent, among the base (Moss and Young 1960; Biegert 1963; Enlow 1990, Lieberman and McCarthy 1999). Therefore, and according to the palimpsest model (Hallgrímsson et al. 2007b; Hallgrímsson and Lieberman 2008), variation in brain growth translates into covariation among the elements that it influences and thus into cranial covariation structure. Given its occurrence during postanatal ontogeny, ACD should be viewed as an external force perturbing this particular developmental process. Therefore, the covariation patterns that are maintained to some extent in our deformed samples should be considered as those more strongly influenced by brain growth during the formation of the cranial vault.

Previous studies comparing altered and non-altered crania from a variety of populations with different kinds of cranial deformation found that changes on the cranial vault were transferred to the face through the cranial base (Cheverud et al. 1992; Kohn et al. 1993). Thus, modifications producing short and wide cranial vaults resulted in short, wide, and shallow faces, while modifications producing long, and narrow cranial vaults resulted in long, narrow, and deep faces (Cheverud et al. 1992; Kohn et al. 1993). Our PLS analyses indicate similar trends, and extend the previous observations to ACD types that had not been fully explored yet using geometric-morphometric methods. Particularly, the shape changes across the first singular vectors (Fig. 3) reflect that covariation among blocks is almost always dominated by the total length and width dimensions of the modules involved, rather than by localized changes; a result which is independently confirmed by the Partial Correlation analyses.

Overall, these tests suggest that there are some aspects of trait covariation (mainly involving size, length, and width of the vault and base) that are significantly correlated simultaneously on different ACD types, regardless of the

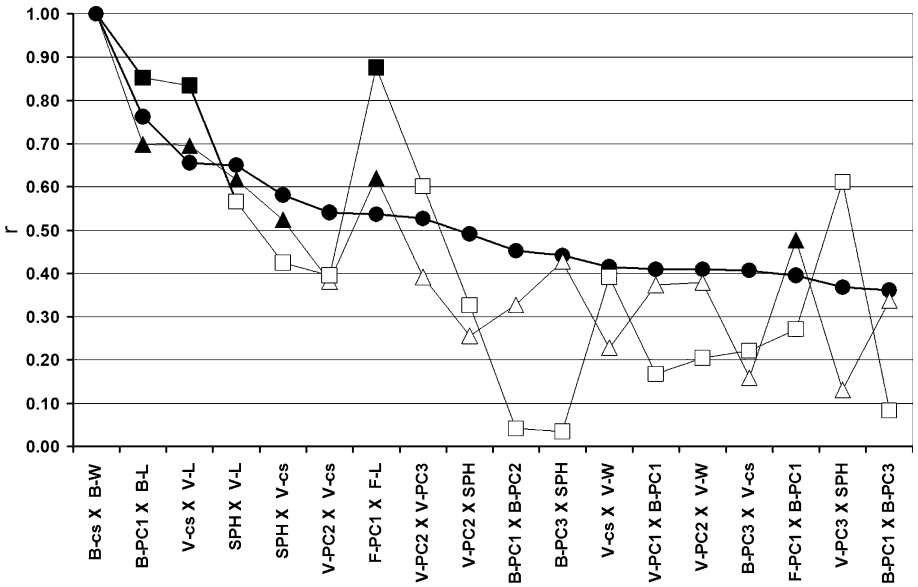

Fig. 5 Partial correlation coefficients among classical measurements and the first three PCs corresponding to each block computed for non-deformed (*circles*), annular (*squares*), and lambdoid flattening (*triangles*) skulls. Results are sorted by decreasing coefficient in the non-deformed series. Filled symbols represent significant coefficients at $\alpha = 0.05$ after Bonferroni's adjustment for 171 comparisons. Empty symbols represent non-significant partial correlations. For simplicity, only significant coefficients for at least one ACD-type are shown. V: vault, F: face, B: base, cs: centroid size, W: relative logarithm of width, L: relative logarithm of length, SPH: sphericity

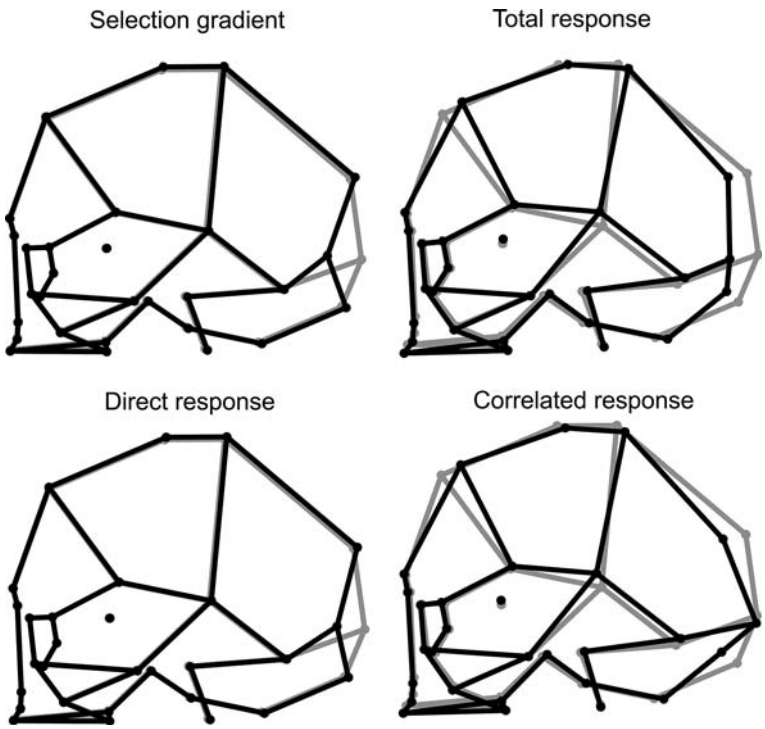

Fig. 6 Hypothetical simulation of lambdoid flattening. The shape changes from the grey wireframe (representing the mean shape of the Hallstatt population) to the black wireframe represent the selection gradient, the total, the direct and the correlated response to selection. Note that the selection gradient was set to ten standard deviations of relative fitness per standard deviation of the respective shape variable

biomechanical strains applied on the skull. Therefore, both PLS and Partial Correlation analyses indicate no rejection of Hn1, and corroborate the observation that some general features of the skull architecture, such as size and relative widths and lengths, are conservative aspects of skull integration that are preserved even under the presence of extreme deformation practices. This is also consistent with previous experimental and comparative studies suggesting that covariation between global skull dimensions (maximum width, length, and centroid size) of adjacent regions is a leading factor on the integration among cranial regions (Weidenreich 1941; Ross and Ravosa 1993; Lieberman

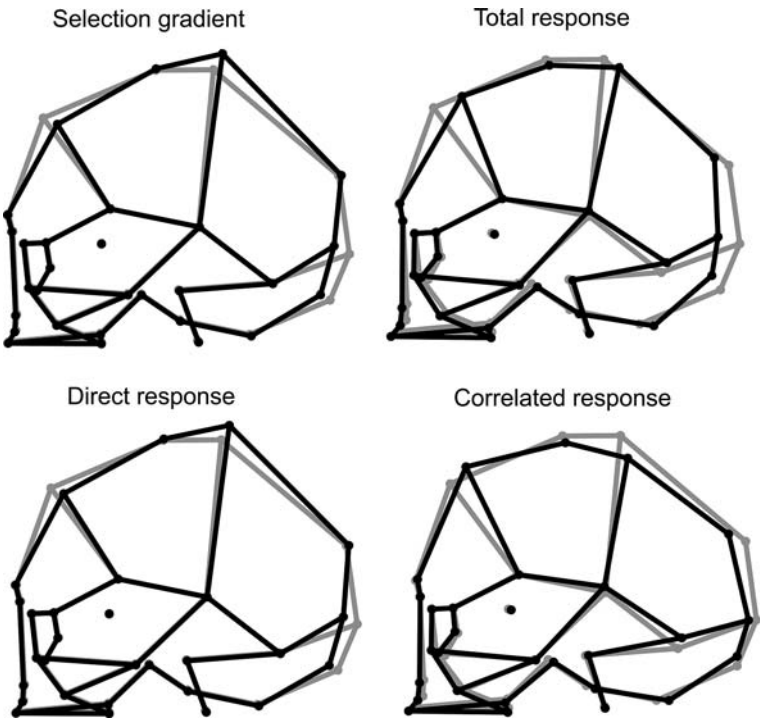

Fig. 7 Hypothetical simulation of annular deformation. For details see Fig. 6

et al. 2000, 2004; Chase et al. 2002; Hallgrímsson et al. 2007a).

Because correlation and covariance structure in our species is stable and largely associated with functional and developmental factors (Cheverud 1996; González-José et al. 2004b), functionally related traits should be highly correlated and, thus, should comprise a single module. This seems to be the most likely explanation to the PLS results which suggest a stronger integration among the cranial vault and the base. In addition, this supports previous findings suggesting that the cranial base and vault act as two linked components of a tightly integrated module (Lieberman et al. 2000, 2004; Hallgrímsson et al. 2007a). This pattern is clearly observed in the ND and LF samples (Fig. 4). Since the growth of the neurocranial structures (both the base and the cranial vault) is mainly driven by the growth of the expanding brain and occurs early during the ontogeny (Sperber 2001), the strong covariation among both structures is not only expected to occur in normal crania, but also in the deformed skulls whose neurocranial growth and development is almost completed when the deformation device is applied (Bastir et al. 2007).

Besides the presence of common trends of covariation observable across the entire spectrum of deformation practices, the results from the ANOVA show significant effects of ACD on almost all classical measurements. The PLS tests suggest that, in general terms, localized strains (e.g. LF) exerted on the vault are not enough to trigger a serious disruption of morphological integration. A previous study made on Hopi samples also demonstrated that this kind of ACD has a significant effect on growth of the cranial vault, but does not affect morphology of the cranial base or the face (Kohn et al. 1995). Conversely, when the ACD device is partially applied on the posterior part of the base (A) or at the anterior portion of the vault (FO), the general pattern of vault-base-face covariation is modified. This result is also apparent from the Partial Correlation analyses, because the LF sample shows stronger similarity with the ND skulls.

In summary, these results indicate non-rejection of the second null hypothesis (Hn2), which expected greater conservation of the "normal" integration pattern in ACD types produced by localized strains. Accordingly, Kohn et al. (1993) showed that annular deformations of the cranial vault produce significant effects on the morphology of the cranial base and face. Similar conclusions arise from experimental vault deformation in mice (Pucciarelli 1978), and studies of premature closure of cranial sutures (Babler et al. 1987), and craniosynostoses (Moss 1959; Kreiborg 1981; Richtsmeier 1987, 1988, 2002). Even when these previous studies focused on absolute morphological differences rather than on covariances among traits, their results are useful to evaluate and compare the degree of localization of the effect of biomechanical different ACD types. In this sense, this and earlier studies confirm that annular deformations exert an important and widespread suite of strains that disrupt not only the absolute shape of the ND skull, but also their pattern of covariation.

As expected, the face is the cranial module less affected by the deformation practices. For instance, the ANOVA analyses detected non-significant facial shape differences among ACD types. Previous experimental studies have suggested that the cranial base operates as a central integrator between the face and the vault (Lieberman et al. 2000, 2004; McCarthy and Lieberman 2001), an idea early introduced by some classical texts by de Beer (1937), Weidenreich (1941), and Biegert (1963). This is supported by the developmental characteristics and the topological position of the base in relation to the vault and the face. The base, for example, is the only part of the skull that grows endochondrally. Moreover, it acts simultaneously as the floor of the neurocranium and the posterior edge of the face. As a consequence, an interesting implication of our results is that the base seems to be acting as a buffer among the region where the strain is applied (the vault, or the base itself), and the face. However, it is interesting to remark that some general dimensions respond to the deformation in a coordinated way across the entire skull, including the facial ones, whereas other aspects of facial shape remain relatively independent.

To sum up, these analyses showed that the human skull is strongly integrated, that the neurocranium behaves as a module and that general dimensions of the skull seem to be developmentally constrained in order to enable the functioning of the skull, even under strong environmental stimuli, such as those exerted by artificial deformation. This shows the underlying potential of response to biomechanical strains of the human skull. Moreover, our results indicate that localized strains of deformation are less disruptive of morphological integration than more generalized forces. This remarks the importance of the type of strains exerted to the skulls (localization and magnitude) as a complex factor influencing normal morphological integration patterns.

Genetic Constraints

An alternative and powerful way to explore constraints is to analyze the structure of the variances and covariances of the **G** matrix (Lande 1979; Cheverud 1984; Arnold et al. 2001; McGuigan 2006). The **G** matrix expresses the pattern of genetic variances and covariances among phenotypic traits, and constraints can be detected by analyzing the **G** matrix using multivariate statistics and quantitative genetic analyses, such as the multivariate version of the breeder's equation (Lande 1979; Lande and Arnold 1983). To explore the particularities of the response to selection contained in the **G** matrix of human craniofacial shape we have simulated two extreme cases paralleling the biomechanical particularities of extreme deformation practices, the generalized annular type, and the localized LF case.

Overall, our results showed that in modern humans skull shape is also strongly integrated at the genetic level. Specifically, they suggest that neurocranial globularity is one of the determinants of human skull shape that is constrained by such genetic integration patterns. This was reflected by the responses to selection obtained after each of the two simulations (Figs. 6, 7), which were both dominated by the correlated response and tended to preserve the globularity of the cranial vault. High genetic correlation among morphological traits, reflected in the genetic covariance matrix, deflected the total response from the originally selected direction of shape change, determined by the selection gradient simulating selection for deformed neurocranial shape (Klingenberg and Leamy 2001).

The structure of the **G** matrix influences the potential evolutionary response to selection (Lande and Arnold 1983; Klingenberg and Leamy 2001; Merilä and Björklund 2004). Indeed, the simulations performed here showed that the responses to selection are canalized to conform to its own inherent shape patterns and to maintain neurocranial globularity (Figs. 6, 7), indicating that departures from normal patterns of neurocranial globularity are genetically constrained (Cheverud 1984).

The effects of simulated changes similar to the deformation practices appear to be relatively minimized by pervasive genetic integration operating on the human skull, since induced changes in the cranial vault, either localized or generalized, generate a global response to selection. Simulations of both LF (Fig. 6), and annular deformation (Fig. 7) produce a response to selection in which neurocranial globularity is, to some extent, always conserved and patterns of morphological integration are not dramatically disrupted. Overall, these results indicate non-rejection of the third null hypothesis (Hn3).

Conclusion

Since there is no straightforward or customary method to detect and measure constraints, we have explored integration patterns at two different levels, the developmental and the genetic one, which differ greatly in its basic assumptions. Whereas our analyses of simulated response to selection reflect intrinsic genetic constraints channeling the way in which the skull reacts against generalized or localized strains, the analyses of morphological integration performed upon artificially deformed skulls help us to detect the morphological aspects that are more tightly correlated during postnatal phases of development. Both mechanisms, along with other processes acting during embryonic development not addressed here, contribute to the bulk of mechanisms and processes that individuals

within a population posses to buffer and canalize their response to environmental fluctuations.

The results obtained in both analyses indicate that there are regular and predictable patterns of covariation on the neurocranium that reflect the underlying potential of response of the modern human skull to biomechanical strains. As a result, it appears that some key neurocranium features, such as size, widths, and lengths operate as constraints which enable the functioning of the skull even under strong environmental stimuli, such as the deformation practice. Moreover, we have detected different responses to forces applied upon the neurocranium that depend on the degree of generalization or localization of the strains. Finally, the pervasiveness of the genetic response to selection suggests significant integration among the higher-order modules of the skull: the face and the neurocranium.

Taking into account all of these results, we conclude that in modern humans neurocranial globularity is a determinant trait in skull shape, which is developmentally and genetically constrained. As it is likely that human evolution was directed towards certain directions of shape change (variation axes) that are genetically and developmentally constrained, neurocranial globularity would represent one of these favored axes of phenotypic variation. This is relevant because neurocranial globularity is one of the main derived characters of modern humans, representing the tendency to produce larger and more globular cranial vaults. This is probably associated with brain enlargement and increased encephalization, which is one of the main processes that led to hominization (Lieberman et al. 2004).

Further research into both experimental and comparative frameworks of morphological integration disturbances due to several epigenetic stimuli will be crucial for the comprehension of the role of channeling and constrains during the evolution of the skull in modern humans.

Acknowledgments We thank to Drs. B. Hallgrímsson, K.E. Willmore and C. Rolian for inviting us to participate in this special number. Two anonymous reviewers provided insightful comments and many helpful suggestions that enhanced this paper. We are also indebted to authorities and museum's curators of the following institutions: Webb's Museum (University of Kentucky, Lexington, USA), Museo de La Plata (University of La Plata, La Plata, Argentina), Parish and Musealverein of Hallstatt (Hallstatt, Austria), Institut für Anatomie (Innsbruck, Austria), and Naturhistorisches Museum Wien and Österreichisches Museum für Volkskunde (Vienna, Austria) for allowing us to measure their valuable cranial collections and for their help during fieldwork. We also want to thank Torstein Sjøvold and Miquel Hernández for their help and support. Finally, we acknowledge Chris Klingenberg for making available MorphoJ. This work was supported by the Wenner Gren Foundation for Anthropological Research, the Universitat de Barcelona, the Spanish Ministerio de Educación y Ciencia MEC-FEDER (CGL2004-00903/BTE), and the Agencia Nacional de Promoción Científica y Tecnológia, Argentina (PICT Jóvenes 20582).

References

Ackermann, R. R., & Cheverud, J. M. (2004). Morphological integration in primate evolution. In M. Pigliucci & K. Preston (Eds.), *Phenotypic integration: Studying the ecology and evolution of complex phenotypes* (pp. 302–319). Oxford: Oxford University Press.

Alberch, P. (1982). Developmental constraints in evolutionary processes. In J. T. Bonner (Ed.), *Evolution and development* (pp. 313–332). Berlin: Springer.

Antón, S. C. (1989). Intentional cranial vault deformation and induced changes of the cranial base and face. *American Journal of Physical Anthropology, 79*, 253–267. doi:10.1002/ajpa.1330790213.

Antón, S. C. (1994). Biomechanical and other perspectives on the Neandertal face. In R. Corruccini & R. Ciochon (Eds.), *Integrated pathways to the past* (pp. 677–695). Englewood Cliffs, NJ: Prentice-Hall.

Antón, S. C., Jaslow, C. R., & Swartz, S. M. (1992). Sutural complexity in artificially deformed human (*Homo sapiens*) crania. *Journal of Morphology, 214*, 321–332. doi:10.1002/jmor.1052140307.

Antón, S. C., & Weinstein, K. J. (1999). Artificial cranial deformation and fossil Australians revisited. *Journal of Human Evolution, 36*, 195–209. doi:10.1006/jhev.1998.0266.

Antonovics, J., & van Tienderen, P. H. (1991). Ontoecogenophyloconstraints? The chaos of constraint terminology. *Trends in Ecology & Evolution, 6*, 166–168. doi:10.1016/0169-5347(91)90059-7.

Arnold, S. J., Pfrender, M. E., & Jones, A. G. (2001). The adaptive landscape as a conceptual bridge between micro- and macroevolution. *Genetica, 112*(113), 9–32. doi:10.1023/A:1013373907708.

Arthur, W. (1997). *The origin of animal body plans: a study in evolutionary developmental biology*. Cambridge: Cambridge University Press.

Atchley, W. R., & Hall, B. K. (1991). A model for development and evolution of complex morphological structures. *Biological Reviews of the Cambridge Philosophical Society, 66*, 101–157. doi:10.1111/j.1469-185X.1991.tb01138.x.

Babler, W. J., Persing, J. A., Nagorsky, M. J., & Jane, J. A. (1987). Restricted growth at the frontonasal suture: alterations in craniofacial growth in rabbits. *The American Journal of Anatomy, 178*, 90–98. doi:10.1002/aja.1001780112.

Bastir, M. (2004). *Análisis de morfometría geométrica de la variación e integración morfológica en el cráneo humano y sus implicaciones para los homínidos de Atapuerca-SH y la evolución de los Neandertales PhD. Dissertation*. Madrid: Universidad Autónoma de Madrid.

Bastir, M., & Rosas, A. (2004). Facial heights: evolutionary relevance of postnatal ontogeny for facial orientation and skull morphology in humans and chimpanzees. *Journal of Human Evolution, 47*, 359–381. doi:10.1016/j.jhevol.2004.08.009.

Bastir, M., & Rosas, A. (2005). Hierarchical nature of morphological integration and modularity in the human posterior face. *American Journal of Physical Anthropology, 128*, 26–34. doi:10.1002/ajpa.20191.

Bastir, M., Rosas, A., & Kuroe, K. (2004). Petrosal orientation and mandibular ramus breadth: Evidence for an integrated petrosomandibular developmental unit. *American Journal of Physical Anthropology, 123*, 340–350. doi:10.1002/ajpa.10313.

Bastir, M., Sobral, P. G., Kuroe, K., & Rosas, A. (2007). Human craniofacial sphericity: A simultaneous analysis of frontal and lateral cephalograms of a Japanese population using geometric morphometrics and partial least squares analysis. *Archives of*

Oral Biology, 53, 295–303. doi:10.1016/j.archoralbio.2007.09.011.

Biegert, J. (1963). The evaluation of characteristics of the skull, hands and feet for primate taxonomy. In S. L. Washburn (Ed.), *Classification and human evolution* (pp. 116–145). Chicago: Aldine.

Bolker, J. A. (2000). Modularity in development and why it matters to evo-devo. *American Zoologist, 40*, 740–776. doi:10.1668/0003-1569(2000)040[0770:MIDAWI]2.0.CO;2.

Bookstein, F. L., Gunz, P., Mitteroecker, P., Prossinger, H., Schaefer, K., & Seidler, H. (2003). Cranial integration in Homo: Singular warps analysis of the midsagittal plane in ontogeny and evolution. *Journal of Human Evolution, 44*, 167–187. doi:10.1016/S0047-2484(02)00201-4.

Buikstra, J. E., & Ubelaker, D. H. (1994). *Standards for data collection from human skeletal remains*. Fayetteville, Arkansas: Arkansas archeological Survey Research Series NO 44.

Chase, K., Carrier, D. R., Alder, F. R., Jarvik, T., Ostrander, E. A., Lorentzen, T. D., et al. (2002). Genetic basis for systems of skeletal quantitative traits: Principal component analysis of the canid skeleton. *Proceedings of the National Academy of Sciences of the United States of America, 99*, 9930–9935. doi:10.1073/pnas.152333099.

Cheverud, J. M. (1984). Quantitative genetics and developmental constraints on evolution by selection. *Journal of Theoretical Biology, 110*, 155–171. doi:10.1016/S0022-5193(84)80050-8.

Cheverud, J. M. (1996). Developmental integration and the evolution of pleiotropy. *American Zoologist, 36*, 44–50.

Cheverud, J. M., Kohn, L. A., Konigsberg, L. W., & Leigh, S. R. (1992). Effects of fronto-occipital artificial cranial vault modification on the cranial base and face. *American Journal of Physical Anthropology, 88*, 323–345. doi:10.1002/ajpa.1330880307.

Collard, M., & Wood, B. A. (2007). Defining the genus Homo. In W. Henke, T. Hardt, & I. Tattersall (Eds.), *Handbook of paleoanthropology* (pp. 1575–1610). Berlin-Heidelberg: Springer.

Day, M. H., & Stringer, C. B. (1982). A reconsideration of the Omo Kibish remains and the erectus-sapiens transition. In 1er Congr Internat Paleont Hum (pp. 814–846). Prétirage. Nice.

Day, M. H., & Stringer, C. B. (1991). Les restes crâniens d'Omo Kibish et leur classification à l'interieur du genre Homo. *L'Anthropologie, 95*, 573–594.

De Beer, G. (1937). *The Development of the Vertebrate Skull*. Oxford: Clarendon Press.

Dembo, A., & Imbelloni, J. (1938). *Deformaciones intencionales del cuerpo humano de carácter étnico*. Buenos Aires: Humanior.

Dryden, I. L., & Mardia, K. V. (1998). *Statistical shape analysis*. Chichester: Wiley.

Enlow, D. (1990). *Facial growth*. Philadelphia: Saunders.

Falconer, D. S., & MacKay, T. F. C. (1996). *Introduction to quantitative genetics*. Longman Group, Ltd: Essex.

González-José, R. (2003). *El poblamiento de la Patagonia. Análisis de la variación craneofacial en el contexto del poblamiento Americano. Ph.D. Dissertation*. Barcelona: Universitat de Barcelona.

González-José, R., Escapa, I., Neves, W. A., Cuneo, R., & Pucciarelli, H. M. (2008). Cladistic analysis of continuous modularized traits provides phylogenetic signals in Homo evolution. *Nature, 453*, 775–778. doi:10.1038/nature06891.

González-José, R., García-Moro, C., Dahinten, S., & Hernández, M. (2002). Origin of Fueguian-Patagonians: an approach to population history and structure using R matrix and matrix permutation methods. *American Journal of Human Biology, 14*, 308–320. doi:10.1002/ajhb.10033.

González-José, R., Martínez-Abadías, N., Van der Molen, S., García-Moro, C., Dahinten, S., & Hernández, M. (2004a). Hipótesis acerca del poblamiento de Tierra del Fuego-Patagonia a partir del análisis genético-poblacional de la variación craneofacial. *Magallania, 32*, 78–79.

González-José, R., Ramírez-Rozzi, F., Sardi, M., Martínez-Abadías, N., Hernández, M., & Pucciarelli, H. M. (2005). Functional-cranial approach to the influence of economic strategy on skull morphology. *American Journal of Physical Anthropology, 128*, 757–771. doi:10.1002/ajpa.20161.

González-José, R., Van der Molen, S., González-Pérez, E., & Hernández, M. (2004b). Patterns of phenotypic covariation and correlation in modern humans as viewed from morphological integration. *American Journal of Physical Anthropology, 123*, 69–77. doi:10.1002/ajpa.10302.

Gould, S. J. (1989). A developmental constraint in *Cerion*, with comments on the definition and interpretation of constraint in evolution. *Evolution; International Journal of Organic Evolution, 43*, 516–539. doi:10.2307/2409056.

Gunz, P., & Harvati, K. (2007). The Neanderthal "chignon": variation, integration, and homology. *Journal of Human Evolution, 52*, 262–274. doi:10.1016/j.jhevol.2006.08.010.

Hall, B. K. (1996). Baupläne, phylotypic stages and constraint. Why are there so few types of animals. In M. K. Hecht (Ed.), *Evolutionary Biology* (Vol. 29, pp. 215–261). New York: Plenum Press.

Hall, B. K. (2005). *Bones and cartilage: Developmental and evolutionary skeletal biology*. San Diego, CA: Elsevier Academic Press.

Hallgrímsson, B., & Lieberman, D. E. (2008). Mouse models and the evolutionary developmental biology of the skull. *Integrative and Comparative Biology, 48*, 373–384. doi:10.1093/icb/icn076.

Hallgrímsson, B., Lieberman, D. E., Liu, W., Ford-Hutchinson, A. F., & Jirik, F. R. (2007a). Epigenetic interactions and the structure of phenotypic variation in the cranium. *Evolution & Development, 9*, 76–91. doi:10.1111/j.1525-142X.2006.00139.x.

Hallgrímsson, B., Lieberman, D. E., Young, N. M., Parsons, T., & Wat, S. (2007b). Evolution of covariance in the mammalian skull. *Novartis Foundation Symposium, 284*, 164–185. doi:10.1002/9780470319390.ch12.

Howells, W. W. (1973). *Cranial variation in man. Papers of the peabody museum of archaeology and ethnology*. Cambridge, Massachusetts, USA: Harvard University.

Jiang, X., Iseki, S., Maxson, R. E., Sucov, H. M., & Morriss-Kay, G. M. (2002). Tissue origins and interactions in the mammalian skull vault. *Developmental Biology, 241*, 106–116. doi:10.1006/dbio.2001.0487.

Klingenberg, C. P. (2005). Developmental constraints, modules, and evolvability. In B. Hallgrímsson & B. K. Hall (Eds.), *Variation. A central concept in biology* (pp. 219–247). San Diego (CA): Elsevier Academic Press.

Klingenberg, C. P. (2008). MorphoJ. Faculty of Life Sciences, University of Manchester, UK. http://www.flywings.org.uk/MorphoJ_page.htm.

Klingenberg, C. P., & Leamy, L. J. (2001). Quantitative genetics of geometric shape in the mouse mandible. *Evolution; International Journal of Organic Evolution, 55*, 2342–2352.

Klingenberg, C. P., Leamy, L. J., Routman, E. J., & Cheverud, J. M. (2001). Genetic architecture of mandible shape in mice: Effects of quantitative trait loci analyzed by geometric morphometrics. *Genetics, 157*, 785–802.

Klingenberg, C. P., & Monteiro, L. R. (2005). Distances and directions in multidimensional shape spaces: implications for morphometric applications. *Systematic Biology, 54*, 678–688. doi:10.1080/10635150590947258.

Kohn, L. A., Leigh, S. R., & Cheverud, J. M. (1995). Asymmetric vault modification in Hopi crania. *American Journal of Physical Anthropology, 98*, 173–195. doi:10.1002/ajpa.1330980207.

Kohn, L. A., Leigh, S. R., Jacobs, S. C., & Cheverud, J. M. (1993). Effects of annular cranial vault modification on the cranial base and face. *American Journal of Physical Anthropology, 90*, 147–168. doi:10.1002/ajpa.1330900203.

Kovac, M., & Groeneveld, E. (2003). VCE-5, User's guide and reference manual. Version 5.1.

Kreiborg, S. (1981). Crouzon syndrome. A clinical and roentgencephalometric study. *Scandinavian Journal of Plastic and Reconstructive Surgery. Supplementum, 18*, 1–198.

Kruuk, L. E. (2004). Estimating genetic parameters in natural populations using the "animal model". *Philosophical Transactions of the Royal Society of London. Series B, Biological Sciences, 359*, 873–890. doi:10.1098/rstb.2003.1437.

Lahr, M. M. (1996). *The evolution of modern human diversity: a study of cranial variation*. Cambridge: Cambridge University Press.

Lande, R. (1979). Quantitative genetic analysis of multivariate evolution, applied to brain: body size allometry. *Evolution; International Journal of Organic Evolution, 33*, 402–416. doi:10.2307/2407630.

Lande, R., & Arnold, S. J. (1983). The measurement of selection on correlated characters. *Evolution; International Journal of Organic Evolution, 37*, 1210–1226. doi:10.2307/2408842.

Lieberman, D. E. (1995). Testing hypotheses about recent human evolution from skulls. *Current Anthropology, 36*, 159–197. doi:10.1086/204348.

Lieberman, D. E. (1997). Making behavioral and phylogenetic inferences from hominid fossils: considering the developmental influence of mechanical forces. *Annual Review of Anthropology, 26*, 185–210. doi:10.1146/annurev.anthro.26.1.185.

Lieberman, D. E., Krovitz, G. E., & McBratney-Owen, B. (2004). Testing hypotheses about tinkering in the fossil record: The case of the human skull. *Journal of Experimental Zoology. Part B. Molecular and Developmental Evolution, 302*, 284–301.

Lieberman, D. E., McBratney, B. M., & Krovitz, G. (2002). The evolution and development of cranial form in Homo sapiens. *Proceedings of the National Academy of Sciences of the United States of America, 99*, 1134–1139. doi:10.1073/pnas.022440799.

Lieberman, D. E., & McCarthy, R. C. (1999). The ontogeny of cranial base angulation in humans and chimpanzees and its implications for reconstructing pharyngeal dimensions. *Journal of Human Evolution, 36*, 487–517. doi:10.1006/jhev.1998.0287.

Lieberman, D. E., Pearson, O. M., & Mowbray, K. M. (2000). Basicranial influence on overall cranial shape. *Journal of Human Evolution, 38*, 291–315. doi:10.1006/jhev.1999.0335.

Luis, M. A., Lustig, A. L., Sardi, M. L., Ponce, P. V., & Pucciarelli, H. M. (1999). Posición de los araucanos en un contexto asiático-europeo II: Metodología Howelliana. *Revista Argentina de Antropología Biológica, 2*, 187–200.

Lynch, J. M., & Walsh, B. (1998). *Genetic analysis of quantitative traits*. Sunderland, MA: Sinauer Associates.

Marroig, G., & Cheverud, J. M. (2005). Size as a line of least evolutionary resistance: diet and adaptive morphological radiation in New World monkeys. *Evolution; International Journal of Organic Evolution, 59*, 1128–1142.

Martínez-Abadías, N. (2007). *Evolutionary patterns of the human skull. A quantitative genetic analysis of craniofacial phenotypic variation. Ph.D. Dissertation*. Barcelona: Universitat de Barcelona.

Maynard Smith, J., Burian, R., Kauffman, S. A., Alberch, P., Campbell, J., Goodwin, B. C., et al. (1985). Developmental constraints and evolution. *The Quarterly Review of Biology, 60*, 265–287. doi:10.1086/414425.

McCarthy, R. C., & Lieberman, D. E. (2001). Posterior maxillary (PM) plane and anterior cranial architecture in primates. *The Anatomical Record, 264*, 247–260. doi:10.1002/ar.1167.

McGuigan, K. (2006). Studying phenotypic evolution using multivariate quantitative genetics. *Molecular Ecology, 15*, 883–896. doi:10.1111/j.1365-294X.2006.02809.x.

Merilä, J., & Björklund, M. (2004). Phenotypic integration as a constraint and adaptation. In M. Pigliucci & K. Preston (Eds.), *Phenotypic integration: Studying the ecology and evolution of complex phenotypes* (pp. 107–129). Oxford: Oxford University Press.

Moss, M. L. (1959). The pathogenesis of premature cranial synostosis in man. *Acta Anatomica, 37*, 351–370. doi:10.1159/000141479.

Moss, M. L. (1968). The primacy of functional matrices in orofacial growth. *Transactions of the British Society of Study of Orthodontics and Dental Practice, 19*, 65–73.

Moss, M., & Young, R. (1960). A functional approach to craniology. *American Journal of Physical Anthropology, 18*, 281–291. doi:10.1002/ajpa.1330180406.

Olson, E. C., & Miller, R. L. (1958). *Morphological integration*. Chicago: University of Chicago Press.

Paschetta, C.A., de Azevedo, S., Castillo, L., Martínez-Abadías, N., Hernández, M., Lieberman, D.E., & González-José, R. (2008). The influence of masticatory loading on craniofacial morphology: A test case across technological transitions in the Ohio Valley (submitted paper).

Pigliucci, M., & Preston, K. (2004). *Phenotypic integration. Studying the ecology and evolution of complex phenotypes*. New York: Oxford University Press.

Ponce de León, M. S., & Zollikofer, C. P. (2001). Neanderthal cranial ontogeny and its implications for late hominid diversity. *Nature, 412*, 534–538. doi:10.1038/35087573.

Pucciarelli, H. M. (1978). The influence of experimental deformation on craniofacial development in rats. *American Journal of Physical Anthropology, 48*, 455–461. doi:10.1002/ajpa.1330480403.

Raff, R. A. (1996). *The shape of life; genes, development and the evolution of animal form*. Chicago: University of Chicago Press.

Richardson, M. K., & Chipman, A. D. (2003). Developmental constraints in a comparative framework: A test case using variations in phalanx number during amniote evolution. *The Journal of Experimental Zoology, 296B*, 8–22. doi:10.1002/jez.b.13.

Richtsmeier, J. T. (1987). Comparative study of normal, Crouzon, and Apert craniofacial morphology using finite element scaling analysis. *American Journal of Physical Anthropology, 74*, 473–493. doi:10.1002/ajpa.1330740407.

Richtsmeier, J. T. (1988). Craniofacial growth in apert syndrome as measured by finite-element scaling analysis. *Acta Anatomica, 133*, 50–56. doi:10.1159/000146614.

Richtsmeier, J. T. (2002). Cranial vault dysmorphology and growth in craniosynostosis. In M. P. Mooney, & M. I. Siegel (Eds.), Understanding craniofacial anomalies. The ethiopathogenesis of craniosynostoses and facial clefting (pp. 321–341). Wiley-Liss.

Rightmire, G. P. (2007). Later middle Pleistocene Homo. In W. Henke, T. Hardt, & I. Tattersall (Eds.), *Handbook of paleoanthropology* (pp. 1695–1715). Berlin-Heidelberg: Springer.

Rohlf, F. J., & Corti, M. (2000). Use of two-block partial least-squares to study covariation in shape. *Systematic Biology, 49*, 740–753. doi:10.1080/106351500750049806.

Rohlf, F. J., & Slice, D. E. (1990). Extensions of Procrustes method for the optimal superimposition of landmarks. *Systematic Zoology, 39*, 40–59. doi:10.2307/2992207.

Ross, C. F., & Ravosa, M. J. (1993). Basicranial flexion, relative brain size, and facial kyphosis in nonhuman primates. *American Journal of Physical Anthropology, 91*, 305–324. doi:10.1002/ajpa.1330910306.

Sardi, M. L., & Pucciarelli, H. M. (2001). Influencia de la deformación artificial indeterminada en las comparaciones

craneanas interpoblacionales. *Revista Argentina de Antropología Biológica, 3*, 23–34.

Schwenk, K. (1995). A utilitarian approach to evolutionary constraint. *Zoology (Jena, Germany), 98*, 251–262.

Sciulli, P. W. (1998). Evolution of the dentition in prehistoric Ohio Valley Native Americans: II. Morphology of the deciduous dentition. *American Journal of Physical Anthropology, 106*, 189–205. doi:10.1002/(SICI)1096-8644(199806)106:2<189::AID-AJPA6>3.0.CO;2-L.

Sciulli, P. W. (2001). Evolution of dentition in prehistoric Ohio Valley Native Americans III. Metrics of deciduous dentition. *American Journal of Physical Anthropology, 116*, 140–153. doi:10.1002/ajpa.1107.

Sheets, H. D. (2004). IMP ThreeDStand6.

Sheets, H. D. (2005). IMP PLS3d.

Sjøvold, T. (1984). A report on the heritability of some cranial measurements and non-metric traits. In G. N. Van Vark & W. W. Howells (Eds.), *Multivariate statistical methods in physical anthropology* (pp. 223–246). Dordrecht: Reidel Publishing Company.

Sjøvold, T. (1995). Testing assumptions for skeletal studies by means of identified skulls from Hallstat, Austria. In S. R. Saunders & A. Herring (Eds.), *Grave reflections: Portraying the past through cemetery studies* (pp. 241–281). Toronto: Canadian Scholars Press Inc.

Sperber, G. (2001). *Craniofacial development*. London: BC Decker Inc.

Steppan, S. J., Phillips, P. C., & Houle, D. (2002). Comparative quantitative genetics: Evolution of the G matrix. *Trends in Ecology & Evolution, 17*, 320–327. doi:10.1016/S0169-5347(02)02505-3.

Strait, D. S. (2001). Integration, phylogeny, and the hominid cranial base. *American Journal of Physical Anthropology, 114*, 273–297. doi:10.1002/ajpa.1041.

Strait, D. S., & Grine, F. E. (2004). Inferring hominoid and early hominid phylogeny using craniodental characters: the role of fossil taxa. *Journal of Human Evolution, 47*, 399–452. doi:10.1016/j.jhevol.2004.08.008.

Strait, D. S., Grine, F. E., & Fleagle, J. G. (2007). Analyzing hominid phylogeny. In W. Henke, T. Hardt, & I. Tattersall (Eds.), *Handbook of paleoanthropology* (pp. 1782–1806). Berlin-Heidelberg: Springer.

Tatarek, N. E., & Sciulli, P. W. (2000). Comparison of population structure in Ohio's late archaic and late prehistoric periods. *American Journal of Physical Anthropology, 112*, 363–376. doi:10.1002/1096-8644(200007)112:3<363::AID-AJPA7>3.0.CO;2-Y.

Tattersall, I. (2002). *The Monkey in the mirror: Essays on the science of what makes us human*. Oxford: Oxford University Press.

Weidenreich, F. (1941). The brain and its role in the phylogenetic transformation of the human skull. *Transactions of the American Philosophical Society, 31*, 320–442. doi:10.2307/1005610.

Wolpoff, M. H. (1980). *Paleoanthropology*. New York: McGraw-Hill.

Zelditch, M. L., Swiderski, D. L., Sheets, H. D., & Fink, W. L. (2004). *Geometric morphometric for biologists*. London: Elsevier Academic Press.